Int J Thermophys (2015) 36:1131–1136
DOI 10.1007/s10765-014-1587-3

Comparative Study of Thermal-Wave Fields in Bi-layered Semi-cylindrical and Fully Cylindrical Solids

Guangxi Xie · Jingpei Hu · Rui Tai · Chinhua Wang · Andreas Mandelis

Received: 3 December 2013 / Accepted: 14 March 2014 / Published online: 2 April 2014

Abstract A theoretical model for characterizing two-layered semi-cylindrical solid samples illuminated with a modulated incident beam on a curved surface using the Green function method is developed. The analytical expression for the thermal-wave (TW) field in such a semi-cylindrical sample is presented. Based on the model, characteristics of the TW field are simulated with different parameters, and comparisons with the whole cylinder model are conducted. It is found that TW properties of semi- and full cylinders show significant differences, especially in the low frequency range. Preliminary experimental validation is also presented with semi-cylindrical samples. The model provides a theoretical basis to quantitatively characterize semi-cylindrical samples using the TW method in a noncontact and nondestructive way.

Keywords Green's function method · Semi-cylindrical samples · Thermal-wave fields

G. Xie
Department of Physics, Jiangnan University, Wuxi 214122, Jiangsu, People's Republic of China

G. Xie · J. Hu · R. Tai · C. Wang (✉)
Institute of Modern Optical Technologies & Collaborative Innovation Center of Suzhou Nano Science and Technology, Jiangsu Key Lab of Advanced Optical Manufacturing Technologies & MOE Key Lab of Modern Optical Technologies, Soochow University, Suzhou 215006, People's Republic of China
e-mail: chinhua.wang@suda.edu.cn

A. Mandelis
Center for Advanced Diffusion-Wave Technologies, Department of Mechanical and Industrial Engineering, University of Toronto, Toronto, ON M5S 3G8, Canada

1 Introduction

Thermal-wave (TW) techniques have become powerful tools for the thermophysical characterization and the nondestructive evaluation of broad classes of materials [1] due to their nondestructive and highly sensitive nature. With increasing applications of TW characterization of materials, studies on curved surface samples (e.g., cylindrical or spherical samples) have been motivated in recent years [2–5]. In practice, manufactured samples with semi-cylindrical or semi-spherical surfaces bounded by a flat surface are often encountered. The effectiveness of the application of the whole cylindrical or spherical models to these semi-cylindrical or semi-spherical samples remains an open question, especially when the radial dimension of the solid is on the order of, or small, compared with the thermal diffusion length. In this work, we develop a theoretical model for characterizing two-layered semi-cylindrical solid samples using the Green function method. The analytical expression for the TW field in such a semi-cylindrical sample is presented. Based on the model, characteristics of the TW fields are simulated with different parameters and comparisons with the full-cylinder model are conducted. Preliminary experimental validation is also presented with semi-cylindrical samples.

2 Theory

The geometry and coordinates of a bi-layered semi-cylinder structure are shown in Fig. 1. The TW field of an infinitely long bi-layered semi-cylindrical solid sample with inner radius a (region I) and outer radius b (region II) can be derived by the Green function method. The thermal conductivity and thermal diffusivity of regions I and II are denoted with (k_1, α_1) and (k_2, α_2), respectively. The harmonic TW equation for the material under investigation in region II can be written as

$$\nabla^2 T(\vec{r}, \omega) - \sigma_2^2(\omega) T(\vec{r}, \omega) = -\frac{1}{k_2} Q(\vec{r}, \omega), \tag{1}$$

where $\sigma_2(\omega) = (\mathrm{i}\omega/\alpha_2)^{1/2} = (1+\mathrm{i})\sqrt{\omega/2\alpha_2}$ is the complex TW number in region II, ω is the angular modulation frequency of the laser beam, and $Q(\vec{r}, \omega)$ is the volume thermal source at coordinates $\vec{r} = (r, \varphi)$ in region II of the material. Based on the

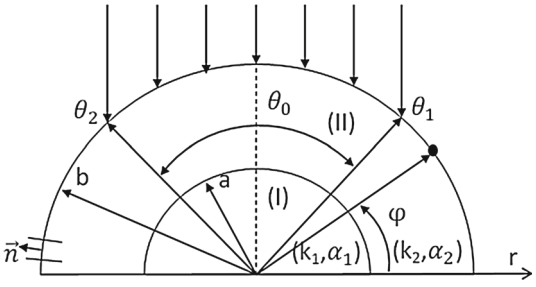

Fig. 1 Cross section of an infinitely long composite half cylinder consisting of two concentric regions of radii a (region I) and b (region II) under external illumination with a uniform light beam impinging on part of its surface subtending a sector of angle θ_0

Green function method, when $Q(\vec{r}_0, \omega) = 0$ (e.g., no volume source in the case of a laser illuminated metal sample), the general solution for Eq. 1 can be written as [6]

$$T(\vec{r}, \omega) = \alpha_2 \oint_{S_0} [G(\vec{r}\,|\vec{r}_0^{\,s}, \omega)\cdot\vec{\nabla}_0 T(\vec{r}_0^{\,s}, \omega) - T(\vec{r}_0^{\,s}, \omega)\cdot\vec{\nabla}_0 G(\vec{r}\,|\vec{r}_0^{\,s}, \omega)]\mathrm{d}\vec{S}_0, \tag{2}$$

where S_0 is the surface surrounding the domain volume V_0 (i.e., region II); $G(\vec{r}|\vec{r}_0, \omega)$ is the TW Green function with units of (s·m^{-3}). We assume a third-kind boundary condition on the inner surface of region II at $r = a$. The homogeneous boundary conditions for the appropriate Green function and inhomogeneous boundary conditions for the temperature field, respectively, can be written as

$$k_2\vec{n}\cdot\nabla G(r\,|\vec{r}_0\,, \omega)\,|_{r=a} = h_1 G(\vec{r}\,|\vec{r}_0\,, \omega)\,|_{r=a} \tag{3a}$$

$$k_2\vec{n}\cdot\nabla G(\vec{r}\,|\vec{r}_0, \omega)\,|_{r=b} = 0 \tag{3b}$$

$$-k_2\vec{n}\cdot\nabla T(\vec{r}\,|\vec{r}_0\,, \omega)\,|_{r=a} = F_1(\vec{r}\,|\vec{r}_0\,, \omega) - h_1 T(\vec{r}\,|\vec{r}_0, \omega)\,|_{r=a} \tag{4a}$$

$$k_2\vec{n}\cdot\nabla T(\vec{r}\,|\vec{r}_0, \omega)\,|_{r=b} = F_2(\vec{r}\,|\vec{r}_0\,, \omega)\,|_{r=b}. \tag{4b}$$

Here h_1 (W·m^{-2}·K^{-1}) is the heat transfer coefficient at the inner surface S_1; F_1 and F_2 are the heat fluxes (W·m^{-2}) imposed on the inner and outer surfaces, respectively. For an axially infinitely long cylinder, the TW field represented by Eq. 2 reduces to

$$\begin{aligned} T(\vec{r}, \omega) = &-\frac{\alpha_2}{k_2}\oint_{S_1} F_1(\vec{r}_0^{\,s}, \omega)\cdot G(\vec{r}\,|\vec{r}_0^{\,s}, \omega)\mathrm{d}S_0 \\ &+\frac{\alpha_2}{k_2}\oint_{S_2} F_2(\vec{r}_0^{\,s}, \omega)\cdot G(\vec{r}\,|\vec{r}_0^{\,s}\,, \omega)\mathrm{d}S_0, \end{aligned} \tag{5}$$

where $G(\vec{r}|\vec{r}_0, \omega)$ is the Green function for region II which must be derived so as to satisfy the appropriate boundary conditions.

As shown in Fig. 1, $F_1 = 0$ when the laser beam is incident on the outer surface, and the TW flux on the curved surface (F_2) must be weighted using a projection factor in the form of the cosine of the incident uniform light intensity. After some algebraic manipulations, the final TW field of a two-layer semi-cylinder can be obtained analytically:

$$\begin{aligned} T(r, \varphi, \omega) = \frac{2F_0}{\pi k_2}\Bigg\{ &2\frac{[K_0(\sigma_2 r) - X_0(a)I_0(\sigma_2 r)]}{I_0'(\sigma_2 b)[Y_0(b) - X_0(a)]}\sin\frac{\theta_0}{2} \\ &+2\sum_{m=1}^{\infty}\frac{[K_{2m}(\sigma_2 r) - X_{2m}(a)I_{2m}(\sigma_2 r)]}{I_{2m}'(\sigma_2 b)[Y_{2m}(b) - X_{2m}(a)]}\cos 2m\varphi\cdot \\ &(-1)^m\left(\frac{\sin(2m+1)\theta_0/2}{2m+1} + \frac{\sin(2m-1)\theta_0/2}{2m-1}\right)\Bigg\} \quad (0 \le \varphi \le \pi), \end{aligned} \tag{6}$$

where

$$X_{2m}(a) = \frac{K'_{2m}(\sigma_2 a) - m_1 K_{2m}(\sigma_2 a)}{I'_{2m}(\sigma_2 a) - m_1 I_{2m}(\sigma_2 a)}, \tag{7}$$

$$Y_{2m}(b) = \frac{K'_{2m}(\sigma_2 b)}{I'_{2m}(\sigma_2 b)}, \tag{8}$$

$$m_1 = \frac{I'_{2m}(\sigma_1 a)}{\beta_{21} I_{2m}(\sigma_1 a)}, \text{ and } \beta_{21} = k_2/k_1, \tag{9}$$

where $I_{2m}(z)$ and $K_{2m}(z)$ are the complex-argument modified Bessel functions of the first kind and of the second kind of order $2m$.

If we set parameter (k_1, α_1) in region I equal to parameters (k_2, α_2) in region II, i.e., $(k_1, \alpha_1) \rightarrow (k_2, \alpha_2)$ in Eq. 9, Eq. 6 can be easily reduced to the single-layer case, i.e., homogeneous semi-cylindrical sample, which can be written as

$$T(r, \varphi, \omega) = \frac{2F_0}{\pi k} \left\{ 2 \frac{I_0(\sigma r)}{I'_0(\sigma b)} \sin \frac{\theta_0}{2} + 2 \sum_{m=1}^{\infty} \frac{I_{2m}(\sigma r)}{I'_{2m}(\sigma b)} \cos 2m\varphi \right.$$
$$\left. (-1)^m \left(\frac{\sin(2m+1)\theta_0/2}{2m+1} + \frac{\sin(2m-1)\theta_0/2}{2m-1} \right) \right\} \quad (0 \le \varphi \le \pi). \tag{10}$$

3 Numerical Calculation

In the following simulations, we assume for simplicity a one-layer sample with either semi-cylindrical or full-cylinder geometry. The amplitude and phase of the surface temperature oscillation are normalized to the corresponding amplitude and phase of a flat surface of a semi-infinitely thick sample of the same material.

Figure 2a1, a2, b1, and b2 shows the effect of the diameter of the semi-cylindrical and full-cylinder samples on the TW field measured at the sample surface ($r = b$) and at an angle of $\varphi = 90°$. Furthermore, $\theta_0 = 180°$ is assumed in the calculations. The other material parameters used in the simulation are as follows: $F_0 = 1\,\mathrm{W{\cdot}m^{-2}}$ and $k = 51.9\,\mathrm{W{\cdot}m^{-1}{\cdot}K^{-1}}$, and $a = 13.57 \times 10^{-6}\,\mathrm{m^2{\cdot}s^{-1}}$ for AISI 1018 carbon steels [7]. From Fig. 2a1, b1, it is seen that both the amplitude and phase of the semi-cylinder show a much larger dynamic range than the full cylinder. This is expected as a result of the higher TW confinement in the former geometry.

Figure 2c1, c2, d1, and d2 shows the effect of the thermal diffusivity of the material on the TW field measured at $\varphi = 90°$ and at illumination angle $\theta_0 = 180°$ for semi-cylindrical and full-cylinder samples, respectively, with a diameter of 3 mm. It is seen that both amplitudes and phases of both geometries are sensitive to the thermal diffusivity, and the peak/valley positions of the amplitude and phase shift toward a higher frequency when the thermal diffusivity increases. The dynamic range of the normalized amplitude and phase of the semi-cylindrical sample are, however, much larger than those of the full-cylinder samples for the same field confinement reason as above.

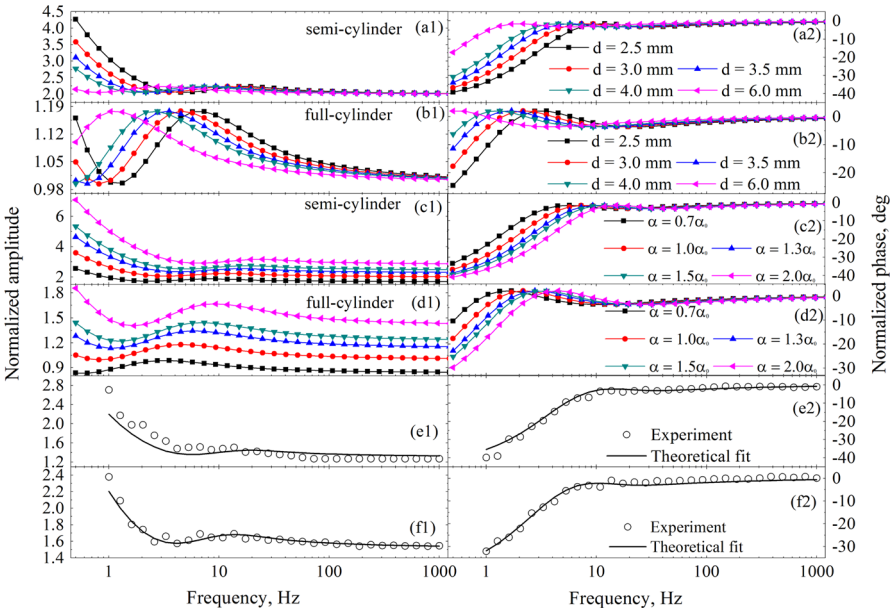

Fig. 2 (a1, a2) and (b1, b2): effect of the diameter of the semi-cylindrical and full- cylinder sample on the TW field measured at the sample surface ($r = b$) and at the angle $\varphi = 90°$. The amplitude and the phase are normalized, respectively, to the corresponding values of a flat surface of the same material; (c1, c2) and (d1, d2): effect of material thermal diffusivity on the normalized surface TW amplitude and phase for half and full cylinder with 3 mm diameter, measured at ($r = b$), $\varphi = 90°$; (e1, e2) and (f1, f2): theoretical best fits to the experimental results; amplitude and the phase for semi-cylindrical steel samples with diameters of 2.5 mm and 3.0 mm, respectively

4 Experimental Results

To verify the foregoing theoretical model, PTR experiments were performed using a series of AISI 1018 semi-cylindrical steel uniform single-layered samples. More details about the PTR experimental setup are available in previous studies [2,3]. All samples were machined to a length of 30 mm, and diameters ranged from 2.5 mm to 6 mm.

Figure 2e1, e2, f1, and f2 shows the experimental results and the corresponding theoretical fits for the aforementioned AISI 1018 semi-cylindrical steel samples (composition: 0.14 % C to 0.2 % C, 0.6 % Mn to 0.9 % Mn) with diameters of 2.5 mm and 3.0 mm, respectively. In the fitting process, the thermal diffusivity of the material and the measurement angle φ are set as the fitting parameters. It is seen that both the amplitude and phase show good agreement between experimental data and the theoretical model. The best-fitted thermal diffusivities are $14.23 \times 10^{-6}\,\mathrm{m^2{\cdot}s^{-1}}$ and $14.60 \times 10^{-6}\,\mathrm{m^2{\cdot}s^{-1}}$, respectively, from Fig. 2e1, e2, f1, and f2. The fitting error can be estimated using the square root of the ratio of the average deviation between the experimental data and the theoretical fits to the normalized amplitude and phase, i.e.,

$$\text{error} = \sqrt{\sum_{i=1}^{2} \frac{\sum_{j=1}^{N} [P_{i,\text{fit}}(f_j) - P_{i,\text{e}}(f_j)]^2}{\sum_{j=1}^{N} [P_{i,\text{e}}(f_j)]^2}},$$

where $i = 1, 2$ represent the amplitude and the phase, respectively. N is the total number of data points (30 points in this case). $P_{i,\text{e}}(f_j)$ is the experimental amplitude and phase, and $P_{i,\text{fit}}(f_j)$ is the amplitude and phase calculated with the theoretical model. The fitting errors for the 2.5 mm and 3 mm diameter semi-cylindrical samples are about 15 % and 11 %, respectively. In the fitting process, we also introduced the measurement angle φ as a fitting parameter to allow us to take into account the actual experimental arrangement in which the laser beam is incident onto the cylindrical surface at a tilted angle [2]. The fitted measurement angle results are $\varphi = 78.7°$ and $79.1°$ for the 2.5 mm and 3 mm diameter semi-cylindrical samples, respectively, which shows the self-consistency of the measurements.

5 Conclusions

In this paper, a theoretical model for characterizing two-layered semi-cylindrical solid samples was established. Based on the model, comparison with the full-cylinder model is made. It is found that the TW fields of half and full cylinders show significant differences, especially in the low frequency range. The experimental results with the semi-cylindrical uniform samples are in good agreement with the theory.

Acknowledgments This work was supported by a grant from the National Natural Science Foundation of China Contract No. 60877063, Scientific Research Foundation for Returned Scholars, Ministry of Education of China, and the project of the Priority Academic Program Development (PAPD) of Jiangsu Higher Education Institutions. The Canada Research Chairs and the Natural Sciences and Engineering Research Council of Canada are gratefully acknowledged for their support through a CRC Tier I award and a Discovery Grant, respectively, to AM.

References

1. D.P. Almond, P.M. Patel, *Photothermal Science and Techniques* (Chapman and Hall, London, 1996)
2. C. Wang, A. Mandelis, L. Liu, J. Appl. Phys. **96**, 3756 (2004)
3. C. Wang, A. Mandelis, Y. Liu, J. Appl. Phys. **97**, 014911 (2005)
4. A. Salazar, R. Celorrio, J. Appl. Phys. **100**, 113535 (2006)
5. N. Madariaga, A. Salazar, J. Appl. Phys. **101**, 103534 (2007)
6. A. Mandelis, *Diffusion-Wave Fields: Mathematical Methods and Green Functions*, Chaps. 2.3, 2.9, 6.19 (Springer, New York, 2001)
7. ASM International, *Metals Handbook*, 10th edn., vol. 1 (ASM International, Materials Park, OH, 1990), p. 196